ACS OMEGA

http://pubs.acs.org/journal/acsodf

Mini-Review

Cavitand and Molecular Cage-Based Porous Organic Polymers

Arkaprabha Giri,* Aniket Sahoo, Tapas Kumar Dutta, and Abhijit Patra*

Cite This: *ACS Omega* 2020, 5, 28413−28424

Read Online

ACCESS | Metrics & More | Article Recommendations

ABSTRACT: Supramolecular cavitands and organic cages having a well-defined cavity and excellent host−guest complexing ability have been explored for a myriad of applications ranging from catalysis to molecular separation to drug delivery. On the other hand, porous organic polymers (POPs) having tunable porosity and a robust network structure have emerged as advanced materials for molecular storage, heterogeneous catalysis, water purification, light harvesting, and energy storage. A fruitful marriage between guest-responsive discrete porous supramolecular hosts and highly porous organic polymers has created a new interface in supramolecular chemistry and materials science, confronting the challenges related to energy and the environment. In this mini-review, we have addressed the recent advances (from 2015 to the middle of 2020) of cavitand and organic cage-based porous organic polymers for sustainable development, including applications in heterogeneous catalysis, CO_2 conversion, micropollutant separation, and heavy metal sequestration from water. We have highlighted the "cavitand/cage-to-framework" design strategy and delineated the future scope of the emerging new class of porous organic networks from "preporous" building blocks.

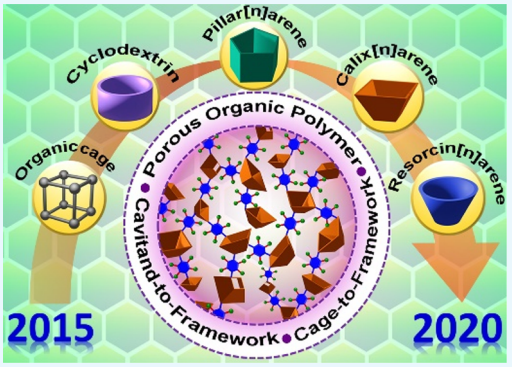

1. INTRODUCTION

Molecular hosts, such as cavitands, capsules, cages, the "Lego" blocks of supramolecular chemistry, having aesthetically appealing architecture, possess large cavities to accommodate small molecules or ions.[1] The confined space of these molecular hosts with excellent guest recognition property leads to multifarious applications ranging from catalysis to molecular separation, sensing, enzyme mimetic catalysis, and development of artificial molecular machines.[1] On the other hand, zeolites, porous carbons, metal−organic frameworks (MOFs), and porous organic polymers (POPs) possess open, continuous one-dimensional (1D) channels or two-dimensional (2D) or three-dimensional (3D) rigid porous networks.[2] Among the aforementioned porous materials, POPs have attracted significant attention in the past few years due to (i) superior chemical, thermal, and hydrothermal stabilities arising from strong covalent bonds, (ii) structural and functional tunability, (iii) lightweight because of B-, C-, N-, O-, and H-based building blocks, and (iv) π-conjugated network structure in conjugated microporous polymers (CMPs).[2b−f]

The intrinsic pores of molecular hosts become isolated (0D pores) in the solid state due to the closed packing, which inhibits facile mass transfer for the bigger substrates.[3] After the guest removal, the supramolecular structures of these molecular hosts are often collapsed. On the other hand, amorphous POPs lack guest selectivity due to the hierarchical pore size distribution. Hence, the marriage of discrete molecular cavitands/cages and polymeric porous organic materials provides a hydrothermally stable robust structure and high porosity, as well as fascinating guest-responsive properties. A new interface of supramolecular chemistry and porous organic materials emerged by knitting the cavitands or cage molecules with suitable aromatic linkers, leading to task-specific POPs with enhanced solid-state guest-responsive properties.

1.1. Cavitand/Cage-to-Framework Design Strategy.

A judicious design strategy for developing a cavitand/cage-based host matrix for solid-state applications is a worthy problem to address. In this regard, various approaches have been demonstrated, such as (i) integrating the cavitands/cages into the supramolecular network polymers through the reversible host−guest interactions,[4a] (ii) fabrication of cavitand/cage-based porous molecular solids through crystallization,[1b] (iii) cross-linking the molecular host through flexible alkyl linkers,[4] and (iv) knitting the molecular containers through covalent linkages with the rigid aromatic linkers.[5] Herein, we focus on the fourth design strategy, where the guest recognition properties and porosity due to the molecular hosts (cavitands, cages) and the rigid aromatic linkers are augmented in the resultant covalently linked network polymers leading to task-specific applications.

Received: August 31, 2020
Accepted: October 20, 2020
Published: October 30, 2020

https://dx.doi.org/10.1021/acsomega.0c04248
ACS Omega 2020, 5, 28413−28424

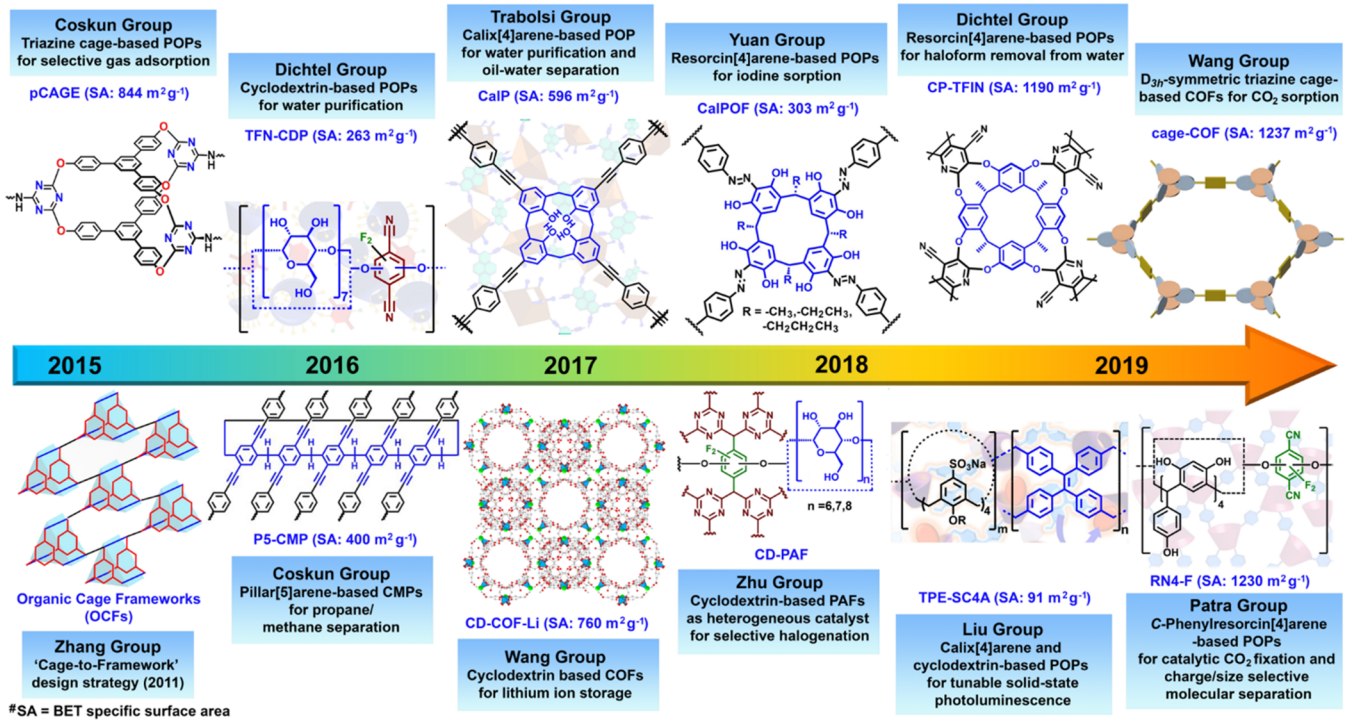

Figure 1. Schematic illustration depicting the progressive development of organic cage and cavitand-based porous organic polymers for multifarious applications. From left to right: first demonstration of "cage-to-framework" design strategy,[5] triazine cage for selective CO_2 adsorption and separation,[7a] β-cyclodextrin-based porous polymer for micropollutant removal from water,[7b] pillar[5]arene-based conjugated microporous polymers for propane/methane separation,[7c] γ-cyclodextrin-based covalent organic frameworks for Li-ion storage,[7d] calix[4]arene-based porous polymer for water purification and oil−water separation,[7e] resorcin[4]arene-based POPs for iodine sequestration,[7f] α,β,γ-cyclodextrin-based postmodified porous aromatic framework for heterogeneous catalysis,[7g] sulfonated calix[4]arene-based POPs for solid-state tuning of photoluminescence,[7h] deep-cavity resorcin[4]arene-based POPs for haloform removal from water,[7i] D_{3h}-symmetric triazine cage for selective CO_2 sorption,[7j] C-phenylresorcin[4]arene-POPs for size/charge-selective molecular separation and, catalytic CO_2 fixation.[7k] CD-COF-Li and cage-COF figures adapted with permission from ref 7d (copyright 2017 John Wiley and Sons) and ref 7j (copyright 2019 American Chemical Society).

In 2011, Zhang and co-workers first demonstrated the strategy for the development of the cross-linked polymers by connecting the "preporous" building blocks such as cages through the covalent attachment (Figure 1).[5] In this approach, porous molecular hosts acting as building blocks are linked with different organic linkers to form the framework. The benefit of the "cavitand/cage-to-framework" strategy is to incorporate the dimensional and functional features of the "preporous" building units into the final framework architecture. A similar design strategy was also discussed in inorganic and hybrid molecular frameworks [e.g., MOFs, polyhedral oligomeric silsesquioxane (POSS) networks, etc.].[6] We restrict our discussion on the recent developments of network polymers derived from all-organic supramolecular building units. Since 2015 onward, various research groups across the globe, such as Dichtel, Coskun, Trabolsi, Yuan, Zhu, Liu, Wang, Patra, and co-workers, have developed a new class of amorphous and crystalline porous organic polymers employing supramolecular cavitands and cages, demonstrating multifunctional applications (Figure 1).[7]

2. CAVITAND-BASED POROUS ORGANIC POLYMERS

According to Cram's definition, cavitands are "synthetic organic compounds that contain enforced cavities large enough to accommodate simple molecules or ions."[8] These "cavities" are constructed by the macrocyclic rings with a range of topologies from concave or bowl-shaped features to fully capsular molecular surfaces. Herein, we have focused our discussion on some of the well-explored bowl-shaped organic cavitands, such as cyclodextrins, calix[n]arenes, calix[4]-resorcinarenes, and pillar[n]arenes, as building blocks for developing crystalline and amorphous POPs.

2.1. Building Block: Cyclodextrin. Cyclodextrins (CDs) have toroidal, rigid structures composed of D-glucopyranose subunits connected by α-1,4-glycosidic bonds.[1a,c] CDs exhibit a high amphiphilicity owing to the outer hydrophilic surface made of a large number of −OH groups and interior hydrophobic cavity with diameters 0.57 (α-CD), 0.78 (β-CD), and 0.95 (γ-CD) nm.[1c,4b] CDs have been heavily explored in supramolecular chemistry due to the excellent host−guest complexation ability.[1a,c,4b] In a pioneering study in 2016, Dichtel and co-workers cross-linked β-CD with rigid aromatic linkers to achieve a mesoporous polymer, TFN-CDP for the sequestration of organic micropollutants from water (Figure 2a).[7b] The use of a rigid aromatic linker, tetrafluoroterephthalonitrile (TFN), instead of conventional flexible cross-linker, epichlorohydrin (EPI), led to the increase in the surface area from 23 (EPI-CDP) to 263 $m^2\ g^{-1}$ (TFN-CDP). The cumulative effect of the host−guest complexation property of β-CD and the mesoporous nature of TFN-CDP resulted in the rapid sequestration of a wide range of organic micropollutants, including microplastic precursors like bisphenol A. The rate of adsorption was 15−200 times higher than that of the well-known carbon-based commercial adsorbents (Brita AC, GAC, NAC) as well as the nonporous β-CD-based polymers (EPI-CDP).[7b] The thermodynamic

https://dx.doi.org/10.1021/acsomega.0c04248
ACS Omega 2020, 5, 28413−28424

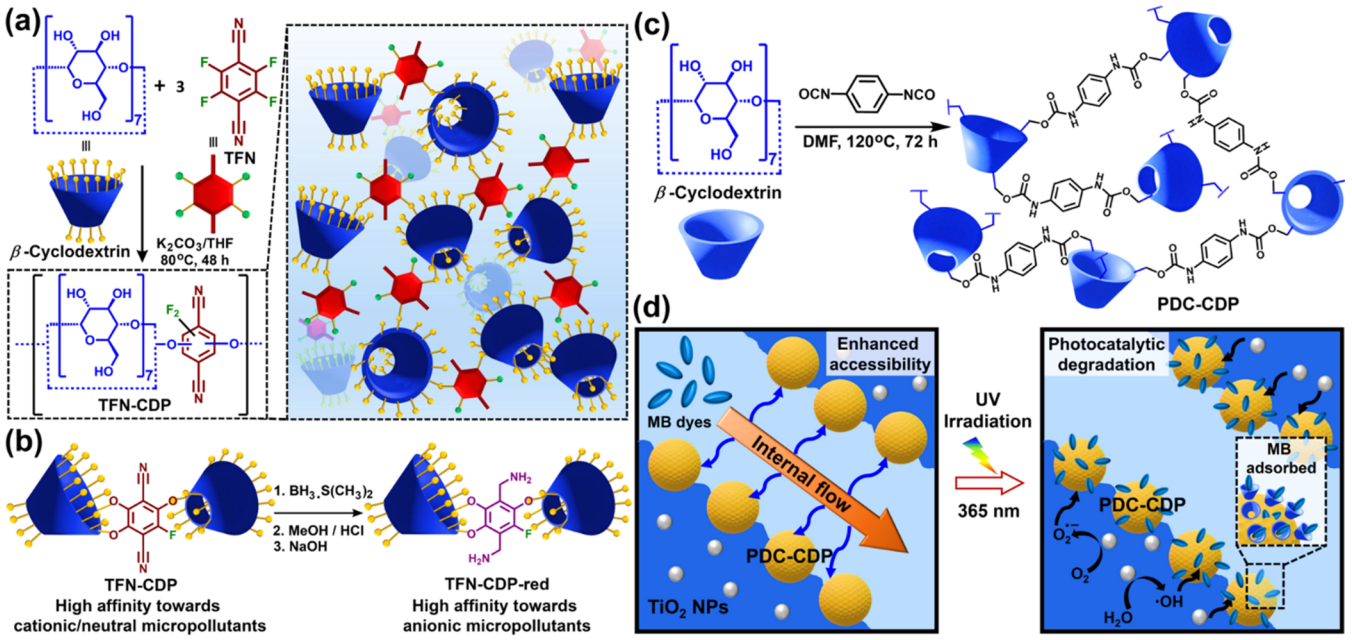

Figure 2. (a) β-Cyclodextrin (β-CD)-based porous organic polymer (TFN-CDP) derived from aromatic nucleophilic substitution reaction (S_NAr) between β-CD and tetrafluoroterephthalonitrile (TFN). Pictorial representation of TFN-CDP polymer (right) employed for micropollutant removal from water. (b) Postsynthetic modification of TFN-CDP polymer (highly selective toward cationic and neutral guests) to amine-functionalized TFN-CDP-red polymer, which shows a high affinity toward anionic guests, including polyfluorinated alkyl substances (PFASs). (c) Schematic representation of PDC-CDP synthesis obtained through the polyaddition reaction between β-CD and 1,4-phenylene diisocyanate (PDC). (d) Plausible mechanism for the rapid sequestration of methylene blue (MB) dye in the hierarchically porous framework (PDC-CDP, left) and photocatalytic degradation of the adsorbed MB dye in the aqueous dispersion of TiO_2-doped PDC-CDP upon photoirradiation at 365 nm (right).

analysis of micropollutant adsorption suggested most of the β-CD units in the polymer can form 1:1 complexes with bisphenol A at equilibrium.

TFN-CDP mostly exhibited a high affinity for cationic and neutral micropollutants.[9a] The formation of anionic phenolate groups through a competing side reaction between TFN and potassium carbonate during the polymerization (zeta-potential: -28.9 ± 0.7 mV) favor adsorption of cationic analytes.[9a] Upon reducing the nitrile groups of TFN-CDP to amines in TFN-CDP-red led to the partial protonation at pH 7 (zeta-potential: $+1.7 \pm 0.8$ mV, Figure 2b). Consequently, TFN-CDP-red showed enhanced binding affinity toward anionic per- and polyfluorinated alkyl substances (PFASs).[9a] In another study, using decafluorobiphenyl as a cross-linker, the Dichtel group developed analogous polymer (DFB-CDP), exhibiting excellent removal efficiency toward PFASs.[9b] The polymerization of β-CD and DFB in a 1:1 ratio led to a nonporous polymer (S_{BET}: <10 $m^2\ g^{-1}$), yet showing performance superior to that of the porous analogue (S_{BET}: 140 $m^2\ g^{-1}$) obtained at different β-CD and DFB ratios. The inferior performance of the cross-linked porous DFB-CDP polymer is consistent with the findings of Karoyo and Wilson, in which heavily substituted β-CD-containing polymers are too sterically hindered to form inclusion complexes.[9c] Recently, β-CD-based adsorbents with tripodal cross-linkers containing either the amino or the amido groups were reported for sequestering PFAS.[9d] The relative importance of the electrostatic interactions and the host−guest interactions due to the respective influence of N-functionalized linkers and β-CD for PFAS binding was explored. These studies demonstrate the crucial role of the chemical functionality of the cross-linkers and cavitand linker ratio for the selective adsorption of organic micropollutants. Additionally, the synergic influence of the "intrinsic porosity" of the cavitand units as well as the "extrinsic porosity" of the cross-linked porous polymers is promising for superior uptake of micropollutants.[7b]

Recently, Chang and co-workers developed a porous polymer (PDC-CDP) by reacting β-CD with 1,4-phenylene diisocyanate (S_{BET}: 171 $m^2\ g^{-1}$, Figure 2c).[10a] The multiscale porous networks (micropores to macropores) were fabricated by employing high-internal-phase emulsion (HIPE) radical polymerization. PDC-CDP rapidly uptakes a variety of organic solvents and adsorbs micropollutants due to the amphiphilic β-CD moieties along with the multiscale porosity (Figure 2d). Upon being embedded with titanium dioxide (TiO_2) nanoparticles, PDC-CDP-HIPE exhibited photocatalytic degradation of organic pollutants with excellent recyclability. The pictorial representation of the catalytic activity indicates the facile mass transport through the internal macrochannels of PDC-CDP-HIPE (Figure 2d). β-CD moieties having a microporous cavity facilitate the rapid uptake of micropollutants. Upon irradiation with UV light (365 nm), the homogeneously distributed TiO_2 nanoparticles produce reactive oxygen species (ROS) to degrade the adsorbed molecules with excellent efficiency.

Cyclodextrins are also well-known as "molecular reaction vessels" for enzyme mimetic catalysis.[1a,c,8] Recently, CD-based porous polymers have emerged as excellent heterogeneous catalysts for selective chemical transformations. Zhu and co-workers prepared a highly fluorinated porous aromatic framework (PAF, S_{BET}: 2436 $m^2\ g^{-1}$) with a hierarchical porosity (Figure 3a).[7g] The postsynthetic covalent modification with different cyclodextrins (α-, β-, γ-CDs) led to CD-PAFs demonstrating selective encapsulation of a diverse range

https://dx.doi.org/10.1021/acsomega.0c04248
ACS Omega 2020, 5, 28413−28424

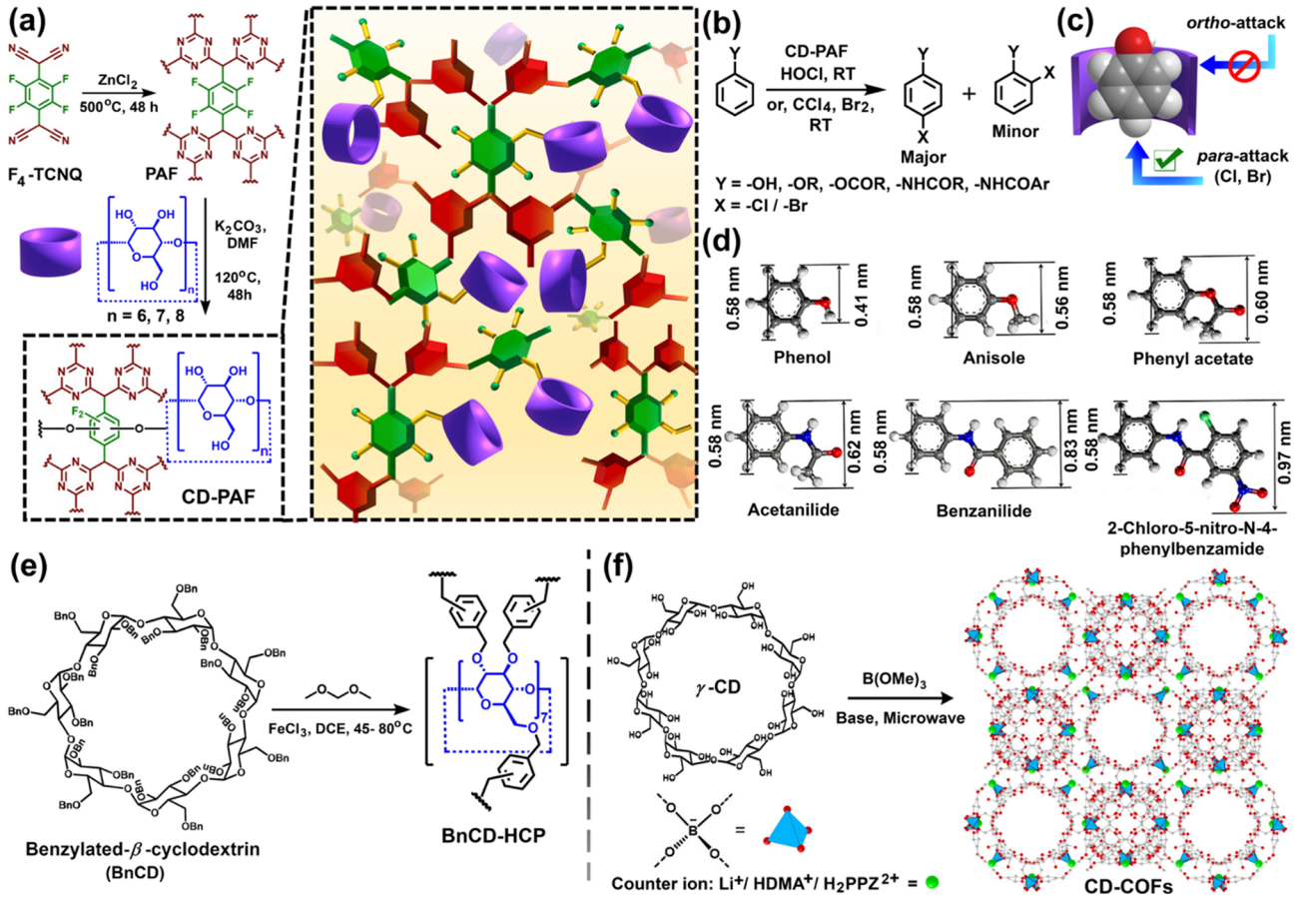

Figure 3. (a) Schematic representation for the synthesis of the porous aromatic framework (PAF) based on tetrafluorotetracyanoquinodimethane (F_4-TCNQ) by an ionothermal process and the postmodification of the resultant PAF through S_NAr reaction with α-, β-, and γ-cyclodextrins, leading to the formation α-CD-PAF, β-CD-PAF, and γ-CD-PAF, respectively, exhibiting high catalytic activity toward regioselective *p*-halogenation of substituted aryl compounds. (b) Reaction scheme of halogenation of diverse aryl compounds catalyzed by CD-PAFs. (c) Pictorial representation of the inclusion complex of phenol and cyclodextrin (only para-position of phenols is accessible for electrophilic substitution upon inclusion to CD-PAF). (d) Molecular dimensions of various aromatic substrates (phenol, anisole, phenylacetate, acetanilide, benzanilide, and 2-chloro-5-nitro-*N*-phenyl benzamide), % of selective *p*-halogenation decreases with increasing substrate size. (e) Schematic representation of β-CD-based hyper-cross-linked polymer (BnCD-HCP) obtained through Friedel–Crafts alkylation using dimethoxy methane as an external cross-linkers; Au nanoparticles-doped BnCD-HCP exhibited high catalytic activity for nitrophenol reduction. (f) Condensation of γ-CD with trimethyl borate($B(OMe)_3$) in the presence of lithium hydroxide (LiOH), dimethylamine (DMA), or piperazine (PPZ) under microwave conditions to afford crystalline γ-CD-covalent organic frameworks (CD-COFs) with different counterions. CD-COFs were employed for selective CO_2 adsorption and Li^+ ion storage. Panels d and f were adapted with permission from ref 7g (copyright 2017 American Chemical Society) and ref 7d (copyright 2017 John Wiley and Sons).

of aryl compounds based on their molecular sizes (Figure 3a–d). α-CD-PAF showed the highest selectivity toward *p*-chlorination over *o*-chlorination compared to β-CD-PAF because of preferential blocking of the *o*-position of the substrates (Figure 3b–d). The selectivity is due to the reduction of cavity size from γ- to α-CD. Again, with the decrease in the substrate size (head diameter: 0.58 nm, tail diameter: 0.97 to 0.41 nm), the uptake capacity of the α-CD-PAF increases (Figure 3d). Pristine PAF did not show any selectivity. On the other hand, only CDs showed good selectivity but poor recyclability. Hence, CD-PAFs bridge the gap between both types of materials, showing excellent selectivity and recyclability. Dai and co-workers developed a highly porous hyper-cross-linked-polymer BnCD-HCP (S_{BET}: 1225 m^2 g^{-1}) through Friedel–Craft alkylation of benzylated β-CD using dimethoxymethane as an external cross-linker (Figure 3e).[10b] The host–guest complexation property of β-CD was used to encapsulate various phenolic pollutants. Further, Au-nanoparticle-doped BnCD-HCP was employed as a heterogeneous catalyst for nitrophenol reduction in water.

Wang and co-workers first developed γ-CD-based covalent organic frameworks (COFs) through a thermodynamically controlled transesterification reaction employing trimethyl borate (Figure 3f).[7d] The use of a 3D preporous building block resulted in the formation of a highly crystalline COF with well-defined nanochannels. The Brunauer–Emmett–Teller (BET) specific surface area was tuned from 494 to 760 to 934 m^2 g^{-1} by exchanging the countercations of negatively charged tetrahedral tetrakis(spiroborate) linkages, respectively, with protonated piperazine ($H2PPZ^{2+}$), Li^+ ion, and protonated dimethylamine ($HDMA^+$) (Figure 3f). A significantly high Li-ion conductivity of 2.7 mS cm^{-1} was observed for CD-COF-Li (20 wt % Li^+) at 30 °C.

2.2. Building Block: Calix[*n*]arene. Calix[*n*]arenes are chalice-like phenol-based cavitands having a hydrophobic cavity with phenolic–OH decorated polar rim.[1a,8] Trabolsi and co-workers first introduced a calix[4]arene cavitand into

https://dx.doi.org/10.1021/acsomega.0c04248
ACS Omega 2020, 5, 28413–28424

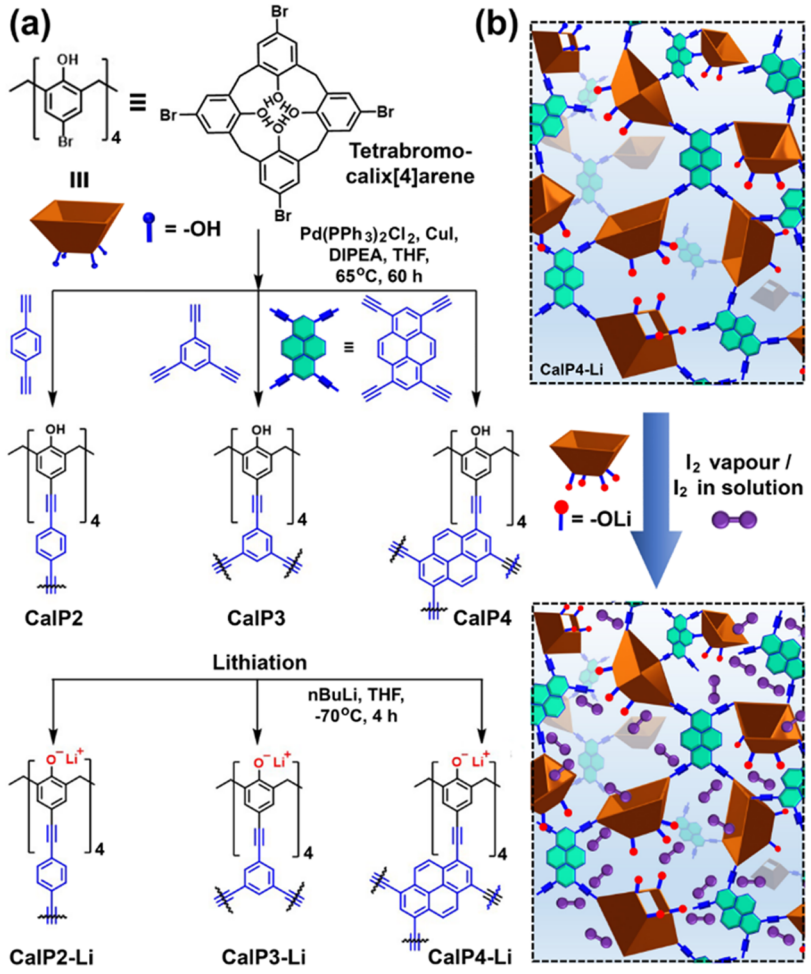

Figure 4. (a) Schematic route for the synthesis of calix[4]arene-based porous organic polymers (POPs) through Sonogashira–Hagihara cross-coupling (CalPs) followed by postsynthetic lithiation of the POPs using *n*-butyl lithium (CalP-Li). (b) Pictorial representation of iodine sequestrations by lithiated polycalix[4]arenes.

the alkyne-linked porous organic polymers (CalPs) in 2017 (Figure 4a).[7e] Pd(II)-catalyzed Sonogashira–Hagihara cross-coupling of tetrabromocalix[4]arene and 1,4-diethynylbenzene led to CalP2 (S_{BET}: 596 m^2 g^{-1}), exhibiting efficient sequestration of organic micropollutants and oil from water. Condensation with tri- and tetra-alkyne-substituted linkers resulted in CalP3 and CalP4 having BET specific surface areas of 630 and 759 m^2 g^{-1}, respectively (Figure 4a).[11a] CalP4 having tetraethynylpyrene linkers showed a bisphenol A uptake rate 2.12 mg g^{-1} min^{-1}, significantly higher than that observed in commercially activated carbons. Various factors were invoked for the high separation efficiency exhibited by CalPs. Phenolic–OH containing a polar rim of calix[4]arene facilitates dipolar and H-bonding interactions with micro-pollutants. The nonpolar electron-rich hydrophobic cavity of calix[4]arene provides a suitable environment to accommodate hydrophobic guests. Additionally, alkyne linkages endow hydrophobicity as well as rigidity to the network to achieve a superhydrophobic highly porous polymer.

Lithiation of the calixarene-based polymers by deprotonating phenolic –OH groups by *n*-butyl lithium led to the ionic porous polymers (Figure 4a).[11b] CalP4-Li showed enhanced iodine capture (312 wt %) attributed to dipole–dipole, ion–dipole, and van der Waals interactions (Figure 4b).[11b] For the sequestration of inorganic pollutants such as heavy metal ions, Hg(II) from water, the Trabolsi group developed a novel cavitand, thioether-crown-calix[4]arene-based porous organic polymers (S-CalP4, S_{BET}: 547 m^2 g^{-1}).[11c] S-CalP4 exhibited an unprecedented high uptake capacity of Hg^{2+} (1686 mg g^{-1}) and fast kinetics, decreasing the mercury level below the acceptable limit for drinking water (2 ppb) within 60 min. The record-high uptake of Hg(II) is due to the high intrinsic sulfur content and soft–soft interactions with thioether-crown-calix[4]arene units.

Trabolsi and co-workers recently demonstrated fine-tuning of the cavitand size of calix[*n*]arenes (*n* = 4, 6, 8) in the POPs governing the removal efficiency of micropollutants, such as the toxic cationic herbicide paraquat (PQ).[11d] Calix[8]arene, having a large cavity size (1.17 nm) along with more effective cation–π interactions with the guest, is likely to be more effective than calix[4]arene (0.3 nm) or calix[6]arene (0.76 nm).

Molecular modeling studies showed the complete inclusion of the cationic PQ in the calix[8]arene. Tetraethynylpyrene and calix[8]arene-based POP, CX8P, exhibited a BET specific surface area (635 m^2 g^{-1}) lower than that of CX4P (759 m^2 g^{-1}) and CX6P (725 m^2 g^{-1}). However, CX8P showed the highest uptake capacity (Q_{max}: 419 mg g^{-1}) with 100% removal of PQ from water in 60 min owing to the exceptional complexation ability.

https://dx.doi.org/10.1021/acsomega.0c04248
ACS Omega 2020, 5, 28413–28424

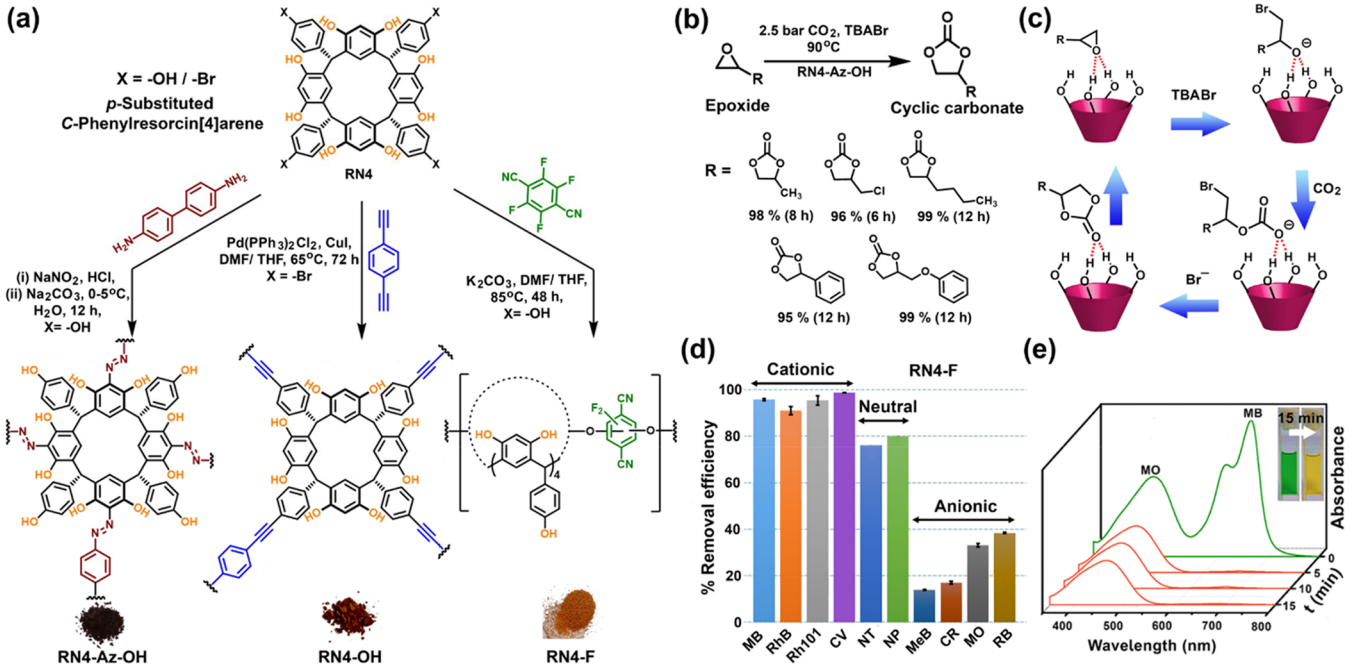

Figure 5. (a) Schematic illustration for the synthesis of *C*-phenylresorcin[4]arene (RN4)-based porous organic polymers: RN4-Az-OH, RN4-OH, and RN4-F through the diazo coupling, Sonogashira cross-coupling, and aromatic nucleophilic substitution reaction, respectively. (b) Conversion of epoxide and CO_2 to cyclic organic carbonates using RN4-Az-OH as a catalyst. (c) Plausible mechanism of the catalytic CO_2 fixation. (d) Size-selective, charge-specific organic dye removal from water by RN4-F polymer (MB, methylene blue; RhB, rhodamine B; Rh101, rhodamine 101; CV, cresyl violet; NT, β-naphthol; NP, 4-nitrophenol; MeB, methyl blue; CR, Congo red; MO, methyl orange; RB, Rose Bengal). (e) Separation of cationic methylene blue from anionic methyl orange. Panels d and e were adapted from ref 7k. Copyright 2019 American Chemical Society.

Liu and co-workers connected sulfonatocalix[4]arenes (SC4A) by tetraphenylethylene derivative (TPE) as a linker (Figure 1).[7h] The resultant mesoporous polymer, TPE-SC4A (S_{BET}: 91 m^2 g^{-1}), showed solid-state photoluminescence (λ_{max}: 500 nm) and guest encapsulation properties. Water-soluble yellow emitting dye 4-[4-(dimethylamino)styryl]-1-methylpyridinium iodide (DASPI, λ_{max}: 580 nm) was encapsulated into the TPE-SC4A polymer matrix. The emission color was tuned from bluish-green to reddish-orange by varying the adsorbed amount of DASPI. Upon excitation of the dye-encapsulated network at 365 nm, two emission peaks around 500 and 580 nm corresponding to TPESC4A and DASPI, respectively, were observed. The peak at 500 nm gradually decreased with concomitant enhancement of the intensity at 580 nm with an increasing amount of DASPI loading due to the fluorescence resonance energy transfer (FRET) from TPE-SC4A to DASPI. Thus, a judicious integration of the photoluminescence property of linkers with guest recognition properties of cavitand units paves the way for exciting development of all-organic solid-state light-harvesting materials.

2.3. Building Block: Resorcin[*n*]arene. Resorcin[*n*]-arenes are a unique class of flexible host, which can change the conformation and cavity size depending on reaction conditions as well as guest molecules.[12] In contrast to calix[4]arene, calix[4]resorcinarene possesses a greater number of phenolic −OH groups that provide multiple propagating sites for polymerization. In 2018, Yuan and co-workers first incorporated a series of *C*-alkylcalix[4]resorcinarene cavitands into the porous organic frameworks (CalPOFs) through facile metal-free diazo coupling reaction (Figure 1).[7f] The BET specific surface areas of calix[4]resorcinarene derivatives with an increase in the alkyl chain length from methyl to ethyl to propyl decreased from 303 to 154 to 91 m^2 g^{-1} for CalPOF-1, CalPOF-2, and CalPOF-3, respectively. The results were anticipated due to the pore-blocking effect associated with the flexible alkyl chains.[7f] The network polymers showed outstanding iodine vapor adsorption capacity with increasing surface area, CalPOF-1 (477 wt %) > CalPOF-2 (406 wt %) > CalPOF-3 (353 wt %). The presence of azo (−N═N−) groups, π-electron-rich cavities, and phenolic −OH units of calix[4]resorcinarene and permanent porous structures contributed to ultrahigh uptake of iodine vapor.

The pore-blocking effect of *C*-alkylresorcin[4]arenes can be circumvented by replacing alkyl groups by rigid aromatic groups in the resorcin[4]arene (RN4) core. Patra and co-workers fabricated a series of RN4-based POPs by employing *C*-phenylresorcin[4]arene derivatives through three different fabrication strategies, such as (i) Pd(II)-catalyzed Sonogashira−Hagihara cross-coupling (RN4-OH), (ii) diazo coupling (RN4-Az−OH), and (iii) aromatic nucleophilic substitution reactions (RN4-F, Figure 5a).[7k] The azo-linked, highly dispersible, hierarchically mesoporous, RN4-Az-OH (S_{BET}: 340 m^2 g^{-1}) exhibited a remarkable catalytic activity with high recyclability for metal-free cycloaddition of CO_2 with a series of epoxides under solvent-free, mild reaction conditions (Figure 5b). The mechanistic investigation revealed the activation of substrate epoxides through H-bonding with phenolic −OH groups of *C*-phenylresorcin[4]arene units (Figure 5c).

Alkyne-linked microporous RN4-OH (S_{BET}: 720 m^2 g^{-1}) showed high H_2 storage capacity (10 mmol g^{-1}, 2 wt %) at 1 bar and 273 K.[7k] The fluorine-rich hydrophobic POP (RN4-F, S_{BET}: 1230 m^2 g^{-1}) exhibited efficient charge-specific and size-selective removal of organic micropollutants from water (Figure 5d).[7k] RN4-F having pore sizes of 0.7 and 1.4 nm

https://dx.doi.org/10.1021/acsomega.0c04248
ACS Omega 2020, 5, 28413−28424

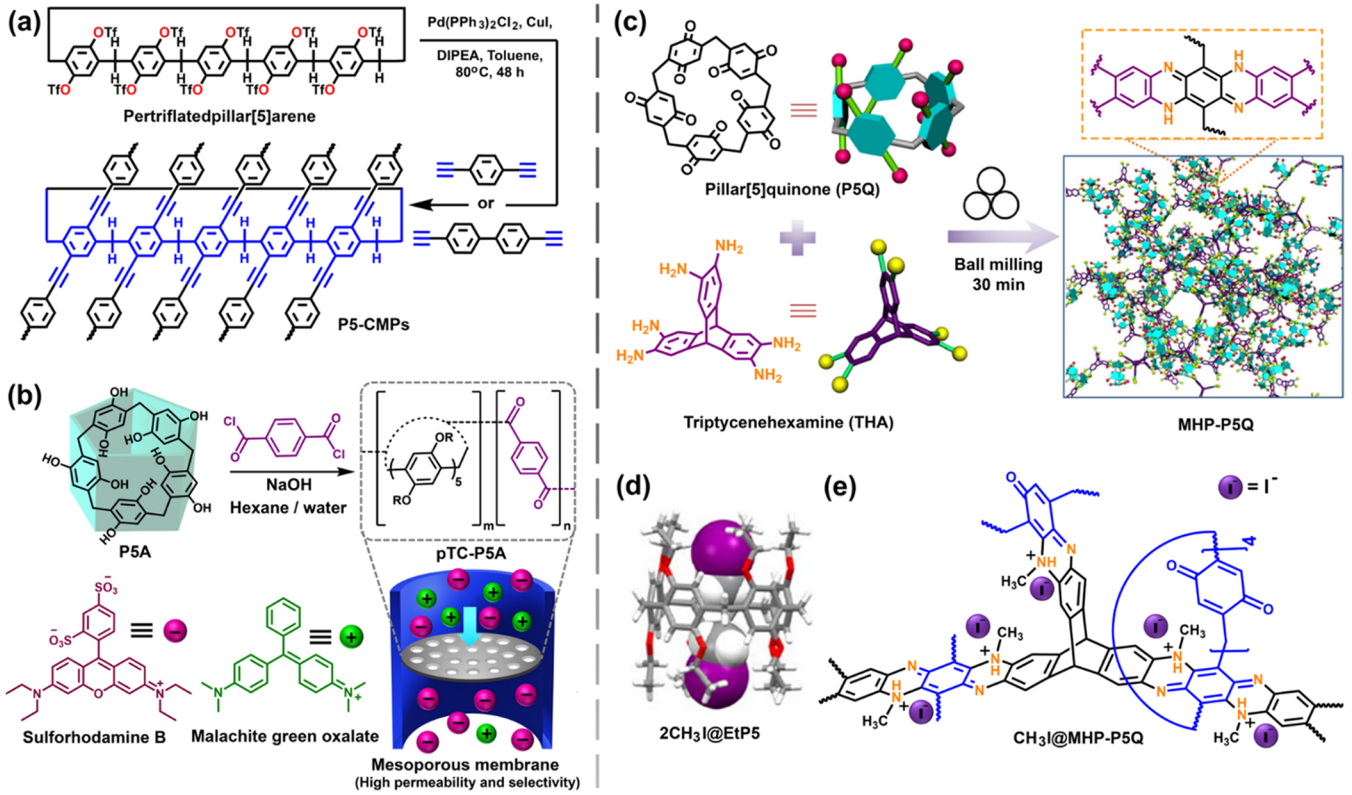

Figure 6. (a) Schematic representation of the synthesis of conjugated microporous polymers based on pillar[5]arene (P5-CMPs) through Sonogashira–Hagihara cross-coupling reaction for propane/methane separation. (b) Synthetic scheme of pillar[5]arene-based porous polymer (pTC-P5A) thin film through interfacial polymerization and charge selective separation of organic dye molecules by pTC-P5A membrane. (c) Mechanochemical synthesis of MHP-P5Q polymer using pillar[5]quinone (P5Q) and triptycenehexamine (THA). (d) Single-crystal X-ray structure of methyl iodide (CH_3I)-loaded perethylated pillar[5]arene ($2CH_3I$@EtP5), indicating encapsulation of two methyl iodide molecules per cavitand. (e) Methylation of amine functionalities on MHP-P5Q during chemisorption process of methyl iodide. Panels c and d were adapted with permission from ref 13b. Copyright 2020 Springer Nature.

effectively adsorbed cationic and neutral micropollutants with comparable molecular dimensions, such as cresyl violet (1.48 × 0.83 nm), methylene blue (1.55 × 0.73 nm), rhodamine B (1.50 × 1.44 nm), rhodamine 101 (1.54 × 1.33 nm), *β*-naphthol (0.82 × 0.62 nm) and *p*-nitrophenol (0.79 × 0.55 nm). On the contrary, larger anionic molecules with multiple charges, such as methyl blue (2.41 × 1.76 nm) and Congo red (2.74 × 0.87 nm), were poorly sequestered. Moreover, RN4-F can selectively separate cationic methyl blue from the equimolar aqueous solution of methyl blue and anionic methyl orange (Figure 5e). Efficient fluorine–cation, *π*–cation, as well as phenolate–cation interactions are assumed to be responsible for the charge-specific molecular separation. In all aspects, RN4-derived POPs outperformed the pristine 0D porous building units in terms of activity as well as recyclability.

Recently, Dichtel and co-workers developed the deep-cavity resorcinarene-based porous organic polymer (CP-TFIN, S_{BET}: 1190 $m^2\ g^{-1}$) employing tetrafluoroisonicotinonitrile (TFIN), believed to be a less sterically hindered linker compared to tetrafluoroterephthalonitrile (TFN), through base-catalyzed nucleophilic aromatic substitution reactions (Figure 1).[7i] Deep-cavity resorcin[*n*]arene derivatives are well-known hosts for various halomethanes and 1,4-dioxane. CP-TFIN was employed for the effective removal of halomethanes and 1,4-dioxane from drinking water. CP-TFIN outperformed commercially available activated carbons and resins in terms of affinity and fast removal kinetics for halomethanes and 1,4-dioxane.

2.4. Building Block: Pillar[*n*]arene. Ogoshi and co-workers in 2008 developed a symmetrical, rigid, and electron-rich supramolecular pillar-shaped cavitand, known as pillar[*n*]arene.[1a] Pillar[5]arene has been explored heavily due to the high yield compared to other pillar[n]arenes. Coskun and co-workers, in 2016, first introduced pillar[5]arene into the alkyne-linked conjugated porous polymers through cross-coupling of triflate substituted pillar[5]arene with 1,4-diethynylbenzene (P5-CMP-1, S_{BET}: 400 $m^2\ g^{-1}$) and 4,4′-diethynyl-1,1′-biphenyl (P5-CMP-2, S_{BET}: 345 $m^2\ g^{-1}$) (Figure 6a).[7c] P5-CMPs exhibit unimodal pore size distribution mainly in the micropore region with a pore diameter of 6 Å. Interestingly, the value is in good agreement with the reported inner cavity of pillar[5]arene. P5-CMP-1 was found to be an excellent material for the separation of propane from a mixture of propane and methane. Intriguing separation of nonpolar gases was due to the matching kinetic length of propane (4.3 Å) with the diameter of the cavity (6 Å) in P5-CMP-1, termed as the "macrocyclic effect".

The guest encapsulation property of pillar[5]arene was further used for the micropollutant removal from the aqueous phase through the fabrication of a semipermeable membrane. A mesoporous membrane (pTC-P5A) with high permeability was designed through interfacial polymerization between benzoyl chloride and pillar[5]arene at the hexane–water interface where the pore dimensions (~3.4 nm) were large enough to facilitate easy movement of the organic/aqueous phase, maintaining the selectivity due to host–guest

https://dx.doi.org/10.1021/acsomega.0c04248
ACS Omega 2020, 5, 28413–28424

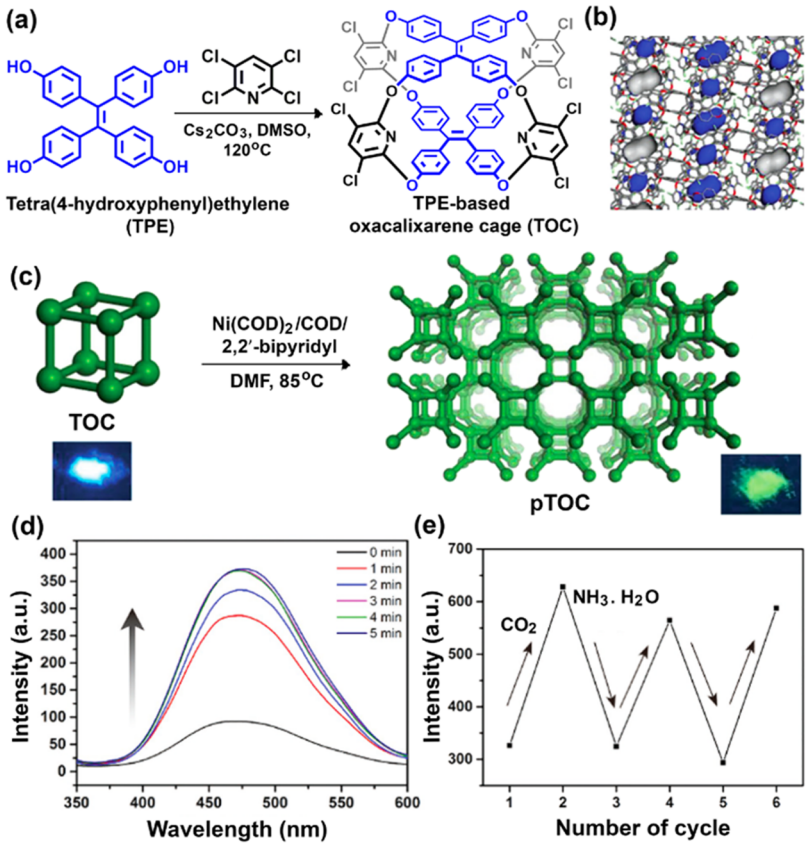

Figure 7. (a) Schematic representation of the synthesis of tetra(4-hydroxyphenyl)ethylene (TPE)-based oxacalixarene cage (TOC). (b) Cross-sectional image of the packing structure of the cage framework suggesting non-interconnected lattice voids in TOC, as illustrated by the blue Connolly surface (probe radius = 1.82 Å). (c) Pictorial representation of the synthesis of the cage-based porous organic polymer (pTOC) through Ni(0)-catalyzed Yamamoto coupling reaction. Inset: Respective digital photographs of TOC and pTOC under the illumination of UV light at 365 nm. (d) Gradual increase in the fluorescence intensity (λ_{ex} = 310 nm) of pTOC by bubbling CO_2 for 0−5 min and (e) recycling tests of pTOC in MeOH upon consecutive bubbling of CO_2 and addition of $NH_3{\cdot}H_2O$. Panels b−e were reprinted in part with permission from ref 15. Copyright 2018 John Wiley and Sons.

interactions involving the cavitand (Figure 6b).[13a] P5A has a specific affinity to cationic guests due to the electron-rich cavity. As shown in Figure 6b, cationic malachite green oxalate was effectively separated from anionic sulforhodamine B by the pTC-P5A film through the nanofiltration of the aqueous solution of the dyes.

Recently, Dai and co-workers demonstrated the mechanochemical synthesis of pillar[5]quinone (P5Q)-derived microporous organic polymers (MHP-P5Q, S_{BET}: 296 $m^2\ g^{-1}$) for removal and storage of CH_3I from the radioactive waste (Figure 6c−e).[13b] The design strategy involves incorporating two rigid building blocks, pillar[5]arene and triptycinehexamine (THA), into the porous 3D network. MHP-P5Q displayed a unique three-step N_2 sorption isotherm with three distinct pore size distributions at 0.76, 1.19, and 1.30 nm. The pore size of 0.76 nm is attributed to the pillar[5]arene intrinsic cavity in the networks. MHP-P5Q was demonstrated to have a superior performance in radioactive iodomethane (CH_3I, 80.3 wt %) capture and storage compared to the analogous network polymer, excluding P5Q (CH3I, 62.2 wt %) and the pristine cavitand perethylated pillar[5]arene (27.6 wt %). The high rate of adsorption of iodomethane in MHP-P5Q is due to the C−H···π intermolecular interactions, leading to efficient host−guest complexation (Figure 6d). The phenazine framework formed an N−CH_3 bond through amine nitrogen (Figure 6e). Additionally, the H_3C−I···N═C− interactions involving the imine functionality of networks stabilized the chemisorptive intermediate. Thus, the synergistic effects of multiple supramolecular forces enhance the adsorption capacity of the cavitand-based POPs.

3. ORGANIC CAGE-BASED POROUS ORGANIC POLYMERS

Shape-persistent organic cages have a rigid regular geometric topology with a well-defined interior, large enough to accommodate guest molecules.[1b] Unlike cavitands, cage molecules have multiple windows that allow the guest molecules to access the intrinsic void space. For example, imine cages have four triangular windows.[1b,d] In the solid state, these cage molecules are closely packed in different alignments, such as window-to-window or window-to-arene.[14] Window-to-window arrangement provides interpore connectivity, leading to porous molecular solid, whereas window-to-arene packing often blocks the intrinsic voids of the cage and limits the diffusion kinetics of the guest molecules. The bottleneck associated with the accessibility of the cage voids in the solid state can be circumvented by the "cage-to-framework" design strategy.[5a] Moreover, the frameworks are also enriched by the guest recognition properties of pristine molecular cages.

Zhang and co-workers first demonstrated the "cage-to-framework" design strategy via Sonogashira cross-coupling between 3D molecular cage and 1,4-diethynylbenzene in 2011

https://dx.doi.org/10.1021/acsomega.0c04248
ACS Omega 2020, 5, 28413−28424

(Figure 1).[5a] The resultant cage-based framework showed CO_2 sorption capacity 4 times higher than that of the pristine cage. Later on, a series of organic cage frameworks (OCFs) through microwave-assisted Sonogashira cross-coupling employing various diacetylene linkers was developed.[5b] Interestingly, the secondary pore volume due to the extrinsic pores (i.e., between the cages) rises with the increase of linker length. It resulted in the amplification of the gas uptake capacity of the OCFs. On the other hand, the linker with a polar electron-rich triethylene glycol methyl ether pendent group endowed strong intermolecular interactions, with CO_2 leading to excellent selective adsorption of CO_2 over N_2 (up to 213/1) at 1 bar and 293 K.[5b] Thus, a judicious choice of linkers with varying sizes and chemical functionalities, and 3D-structure imparted due to the cage alter the gas adsorption property and selectivity of the frameworks.

Coskun and co-workers fabricated a series of porous cage frameworks (pCAGEs) using a shape-persistent triazine cage as a building block through a catalyst-free polymerization route. The frameworks, pCAGE-1 (S_{BET}: 629 m^2 g^{-1}), pCAGE-2 (S_{BET}: 711 m^2 g^{-1}), and pCAGE-3 (S_{BET}: 844 m^2 g^{-1}), were obtained by varying the size and topology of the linkers, namely, hydrazine (1D), 1,3,5-tri(4-aminophenyl) benzene (2D), and tetrakis(4-aminophenyl)adamantane (3D), respectively (Figure 1).[7a] Owing to the triazine moieties in the building units, the pCAGEs showed superior affinity toward CO_2 adsorption (up to 4.2 mmol g^{-1}, 18.5 wt % at 1 bar, 273 K) with a Q_{st} value of 42.9 kJ mol^{-1} at high loading. The affinity of pCAGEs toward CO_2 arises from ultramicroporosity, i.e., the intrinsic porosity of triazine cage building blocks termed "cage effect". A control network using a "half-CAGE" molecule (without having the cage void) as a monomeric unit was synthesized. The resulting polymer showed a Q_{st} value (25.2 kJ mol^{-1}) substantially lower than that of the pristine CAGE (39.4 kJ mol^{-1}) as well as pCAGEs, indicating the importance of the cage effect.[7a]

Zhang and co-workers synthesized a fluorescent cage-based polymeric framework (pTOC) by using tetraphenylethylene-based oxacalixarene cage (TOC) via nickel (0)-catalyzed Yamamoto-type Ullmann coupling reaction (Figure 7).[15] In TOC, the two propeller-like TPE units are fixed by four pyridine units through oxo bridges, resulting in a quadrangular prismatic cage structure (Figure 7a). The TOC showed "window-to-arene" packing mode in the solid state, leading to nonconnective lattice voids (illustrated by the blue Connolly surface, Figure 7b).[14] The packing mode of TOC resulted in a nonporous crystalline solid (S_{BET}: 8 m^2 g^{-1}). However, knitting the discrete cage molecules by covalent bonds into a framework structure gave rise to pTOC. Resolving the issue of "window-to-arene" stacking, pTOC exhibited permanent porosity with a high BET specific surface area (929 m^2 g^{-1}). pTOC showed a high CO_2 uptake capacity of 49.3 cm^3 g^{-1} (9.7 wt %) at 273 K, 1 bar, and strong green fluorescence under excitation of UV light at 365 nm (Figure 7c). Upon bubbling CO_2 into the methanolic dispersion of pTOC for 5 min led to 307% enhancement in the fluorescence (Figure 7d). CO_2 molecules (kinetic diameter: 3.3 Å) are able to fit into the cavities (5.8 Å) of pTOC and interact with heteroatoms in the cage skeleton through local dipole/quadrupole interactions. Hence, the rotation and vibration of phenyl rings of the TPE moieties are further restricted, blocking the nonradiative decay channels, resulting in fluorescence enhancement. Again, after the addition of $NH_3 \cdot H_2O$ into the dispersion, CO_2 was removed from the cavity, and the initial fluorescence intensity of pTOC was regained (Figure 7e).

Wang and co-workers synthesized the extended crystalline COFs using porous organic cages as building units (Figure 8).[7j] The rigid, D_{3h}-symmetric triazine-based molecular cage

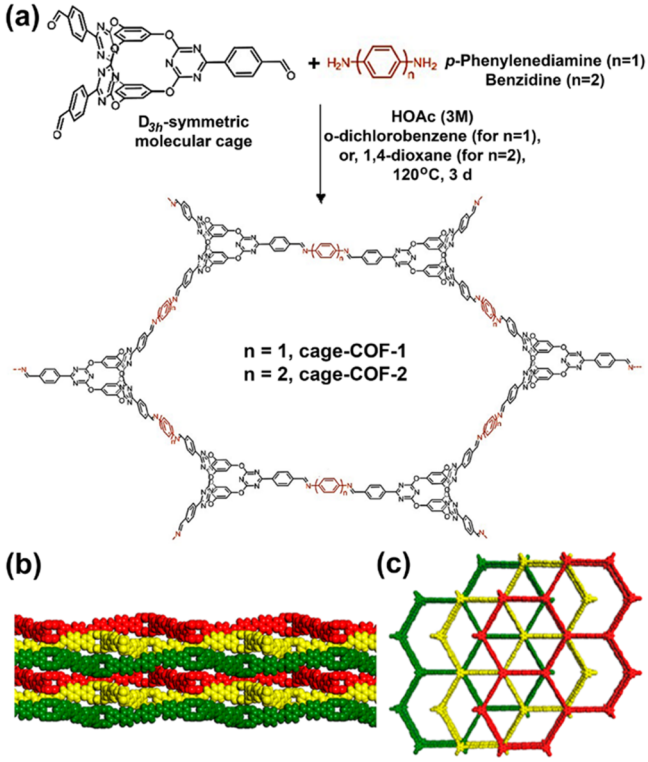

Figure 8. (a) Schematic representation of the synthesis of molecular cage-based crystalline covalent organic frameworks (cage-COFs) by reacting D_{3h}-symmetric organic cage with *p*-phenylenediamine and benzidine through acid-catalyzed Schiff base condensation. Structural representations for (b) side and (c) top view of cage-COF-1. Reprinted from ref 7j. Copyright 2019 American Chemical Society.

consists of three V-shaped electron-deficient cavities. The hexagonal COF skeletons were fabricated taking the cage as a C_3-symmetric knot with *p*-phenylenediamine and benzidine as linkers for cage-COF-1 (S_{BET}: 1237 m^2 g^{-1}) and cage-COF-2 (S_{BET}: 667 m^2 g^{-1}), respectively (Figure 8a). The unique structure of cage COFs originated due to the antidirectional diimine linkages with vertically aligned aromatic linkers, resulting in a rippled layer with staggered ABC packing (Figure 8b,c). Integration of triazine cages into the crystalline frameworks led to the significantly high CO_2 uptake of 43.8 (8.6 wt %) and 37.3 cm^3 g^{-1} (7.3 wt %) for cage-COF-1 and cage-COF-2, respectively, at 273 K and 1 bar. Integrating the shape-persistent preporous organic cages into the crystalline porous frameworks via dynamic covalent chemistry is promising for cooperative sorption with enhanced efficiency and selectivity.[16]

Recently, Cooper and co-workers introduced a trigonal prismatic cage (Cage-6-NH2) as a novel 3D building block with six propagating sites for the construction of the 3D imine linked COF.[17] The cage-based 3D COF (3D-CageCOF-1, S_{BET}: 1040 m^2 g^{-1}) adopts an unprecedented topology with a two-fold interpenetration. Due to the flexibility in the cage knot, 3D-CageCOF-1 showed unique reversible switching between a large-pore structure and a small-pore structure in

https://dx.doi.org/10.1021/acsomega.0c04248
ACS Omega 2020, 5, 28413−28424

the presence and absence of dimethylformamide, respectively. The presence of a N,O-decorated backbone with hydrophilic pore environment helped to harvest water with a maximum capacity of 33 wt % at low humidity conditions (<40%) at 298 K.

4. FUTURE SCOPE AND CONCLUSION

The present mini-review sheds light on various aspects of supramolecular hosts as building units for developing amorphous and crystalline porous organic materials. We presented the whole gamut of recent research based on the structure−property relationship of supramolecular host-based POPs for task-specific applications, such as selective gas adsorption, water purification, heavy metal sequestration, as well as heterogeneous catalysis. Since the genesis, we have witnessed excellent progress in the field in the last 5 years. However, there are considerable scopes to employ these materials for state-of-the-art applications.

(i) Some cavitands/cages, even though having excellent guest recognition properties, are seldom used for polymerization either due to their multistep synthetic routes with low yields or because they lack suitable functionalities for polymerization. Therefore, introducing well-crafted, green, and high-yielding fabrication methodology is desirable to integrate novel cavitand/cage-building blocks into the porous polymers. We envision cucurbit[*n*]urils, tubularenes, imine cages, porphyrin boxes, etc. to have tremendous application potential as building units in the near future.

(ii) Processability is a bottleneck for the cavitand/cage-based POPs in real-time applications. Making the cavitand/cage-based polymers solution-processable and retaining their porosity is a formidable challenge. Such processable POPs may find novel applications in light harvesting, surface coating, and dip catalysis, etc.[18] Cavitand/cage-based POPs not only sequester toxic pollutants from the aqueous phase but also can be used in protective equipment, such as in masks to filter the air from toxic gases, volatile organic compounds,[19] and microbes.

(iii) Development of innovative design strategies for supramolecular host-based POPs to augment guest-responsive property and porosity for the fabrication of drug delivery vehicles, stimuli-responsive smart materials, sensors, and artificial molecular machines to enzyme mimetic catalysis are some of the exciting avenues for further research.

Recent studies on cavitand/cage-based POPs, as outlined in this mini-review, provide numerous promising scopes for sustainable developments, including environmental remediation. Thus, the emerging class of materials stemmed from the marriage of molecular container and porous polymer, if explored adequately, can turn out to be the "materials for tomorrow".

AUTHOR INFORMATION

Corresponding Authors

Arkaprabha Giri − *Indian Institute of Science Education and Research Bhopal, Bhopal 462066, Madhya Pradesh, India;* orcid.org/0000-0003-4356-2014; Email: arkaprabha16@iiserb.ac.in

Abhijit Patra − *Indian Institute of Science Education and Research Bhopal, Bhopal 462066, Madhya Pradesh, India;* orcid.org/0000-0003-3144-1813; Email: abhijit@iiserb.ac.in

Authors

Aniket Sahoo − *Indian Institute of Science Education and Research Bhopal, Bhopal 462066, Madhya Pradesh, India*

Tapas Kumar Dutta − *Indian Institute of Science Education and Research Bhopal, Bhopal 462066, Madhya Pradesh, India;* orcid.org/0000-0001-6431-2060

Complete contact information is available at: https://pubs.acs.org/10.1021/acsomega.0c04248

Author Contributions

The manuscript was written through contributions of all authors. A.G. and A.P. framed and organized the manuscript.

Funding

DST/CHM/2018/086 (DST/TM/WTI/WIC/2K17/82(G), SERB/CHM/2017/113 (File No. EMR/2017/000233), and MHRD STARS/APR2019/CS/560/FS.

Notes

The authors declare no competing financial interest.

Biographies

Arkaprabha Giri is from West Bengal, India. He completed his B.Sc. degree in Chemistry from Bajkul Milani Mahavidyalaya in 2013 and M.Sc. degree from Vidyasagar University in 2015. In 2016, he joined for a Ph.D. under the supervision of Dr. Abhijit Patra at the Indian Institute of Science Education and Research Bhopal. He is interested in developing cavitand-based porous organic polymers for catalytic CO_2 fixation and water purification.

Aniket Sahoo is from Kolkata, West Bengal. He completed his B.Sc. in Chemistry from Asutosh College, Kolkata (University of Calcutta, 2016). He received his M.Sc. degree in Chemistry from Tezpur University, Assam, in 2018. In 2019, he joined the Indian Institute of Science Education and Research Bhopal to pursue a Ph.D. under the guidance of Dr. Abhijit Patra. His research work focuses on

https://dx.doi.org/10.1021/acsomega.0c04248
ACS Omega 2020, 5, 28413−28424

developing the functional porous organic framework and cavitand-based material for heavy metal sequestration and wastewater management.

Tapas Kumar Dutta is from Purulia, West Bengal, India. He completed his B.Sc. in Chemistry from J.K. College, Purulia (Sidho-Kanho-Birsha University, Purulia, 2015), followed by M.Sc. in Physical Chemistry from Banaras Hindu University (Varanasi) in 2017. He joined the Indian Institute of Science Education and Research Bhopal in 2018 to pursue his doctoral program. His research interest is covalent organic frameworks as energy storage materials.

Abhijit Patra studied chemistry at Burdwan University and received his Ph.D. in 2009 from the University of Hyderabad for Research in molecular nano/microcrystals with Prof. T.P. Radhakrishnan as a supervisor. After postdoctoral research at PPSM, ENS Paris-Saclay, and the University of Wuppertal as an Alexander von Humboldt fellow, he started his research career in 2012 at the Indian Institute of Science Education and Research Bhopal. His research interests are multifunctional porous polymers for carbon dioxide conversion, water purification, photocatalysis, light harvesting and energy storage, and optical materials based on molecular and polymeric assemblies at nano/microscale.

■ ACKNOWLEDGMENTS

Financial support from DST-SERB and infrastructural support from IISER Bhopal are gratefully acknowledged. A.G. thanks UGC, and A.S. and T.K.D. thank IISERB for fellowships.

■ REFERENCES

(1) (a) Ogoshi, T.; Yamagishi, T.; Nakamoto, Y. Pillar-Shaped Macrocyclic Hosts Pillar[n]arenes: New Key Players for Supramolecular Chemistry. *Chem. Rev.* **2016**, *116*, 7937−8002. (b) Hasell, T.; Cooper, A. I. Porous Organic Cages: Soluble, Modular and Molecular Pores. *Nat. Rev. Mater.* **2016**, *1*, 16053. (c) Uekama, K.; Hirayama, F.; Irie, T. Cyclodextrin Drug Carrier Systems. *Chem. Rev.* **1998**, *98*, 2045−2076. (d) Hussain, W. M.; Giri, A.; Patra, A. Organic Nanocages: A Promising Testbed for Catalytic CO_2 Conversion. *Sustainable Energy Fuels* **2019**, *3*, 2567−2571. (e) Ortiz, M.; Cho, S.; Niklas, J.; Kim, S.; Poluektov, O. G.; Zhang, W.; Rumbles, G.; Park, J. Through-Space Ultrafast Photoinduced Electron Transfer Dynamics of a C70-Encapsulated Bisporphyrin Covalent Organic Polyhedron in a Low-Dielectric Medium. *J. Am. Chem. Soc.* **2017**, *139*, 4286−4289. (f) Qiu, L.; McCaffrey, R.; Jin, Y.; Gong, Y.; Hu, Y.; Sun, H.; Park, W.; Zhang, W. Cage-templated Synthesis of Highly Stable Palladium Nanoparticles and Their Catalytic Activities in Suzuki-Miyaura Coupling. *Chem. Sci.* **2018**, *9*, 676−680. (g) Sun, N.; Wang, C.; Wang, H.; Yang, L.; Jin, P.; Zhang, W.; Jiang, J. Multifunctional Tubular Organic Cage-Supported Ultrafine Palladium Nanoparticles for Sequential Catalysis. *Angew. Chem., Int. Ed.* **2019**, *58*, 18011−18016.

(2) (a) Furukawa, H.; Cordova, K. E.; O'Keeffe, M.; Yaghi, O. M. The Chemistry and Applications of Metal-Organic Frameworks. *Science* **2013**, *341*, 1230444. (b) Thomas, A. Functional Materials: From Hard to Soft Porous Frameworks. *Angew. Chem., Int. Ed.* **2010**, *49*, 8328−8344. (c) Patra, A.; Scherf, U. Fluorescent Microporous Organic Polymers: Potential Testbed for Optical Applications. *Chem. - Eur. J.* **2012**, *18*, 10074−10080. (d) Xu, Y.; Jin, S.; Xu, H.; Nagai, A.; Jiang, D. Conjugated Microporous Polymers: Design, Synthesis and Application. *Chem. Soc. Rev.* **2013**, *42*, 8012−8031. (e) Slater, A. G.; Cooper, A. I. Function-led Design of New Porous Materials. *Science* **2015**, *348*, No. aaa8075. (f) Hussain, W. M.; Bhardwaj, V.; Giri, A.; Chande, A.; Patra, A. Multifunctional Ionic Porous Frameworks for CO_2 Conversion and Combating Microbes. *Chem. Sci.* **2020**, *11*, 7910−7920.

(3) Tian, J.; Thallapally, P. K.; McGrail, B. P. Porous Organic Molecular Materials. *CrystEngComm* **2012**, *14*, 1909−1919.

(4) (a) Xia, D.; Wang, P.; Ji, X.; Khashab, N. M.; Sessler, J. L.; Huang, F. Functional Supramolecular Polymeric Networks: The Marriage of Covalent Polymers and Macrocycle-Based Host-Guest Interactions. *Chem. Rev.* **2020**, *120*, 6070−6123. (b) van de Manakker, F.; Vermonden, T.; van Nostrum, C. F.; Hennink, W. E. Cyclodextrin-Based Polymeric Materials: Synthesis, Properties, and Pharmaceutical/ Biomedical Applications. *Biomacromolecules* **2009**, *10*, 3157−3175.

(5) (a) Jin, Y.; Voss, B. A.; Jin, A.; Long, H.; Noble, R. D.; Zhang, W. Highly CO_2-Selective Organic Molecular Cages: What Determines the CO_2 Selectivity. *J. Am. Chem. Soc.* **2011**, *133*, 6650−665. (b) Jin, Y.; Voss, B. A.; McCaffrey, R.; Baggett, C. T.; Noble, R. D.; Zhang, W. Microwave-assisted Syntheses of Highly CO_2-selective Organic Cage Frameworks (OCFs). *Chem. Sci.* **2012**, *3*, 874−877.

(6) (a) Inokuma, Y.; Arai, T.; Fujita, M. Networked Molecular Cages as Crystalline Sponges for Fullerenes and Other Guests. *Nat. Chem.* **2010**, *2*, 780−783. (b) Wang, S.; Tan, L.; Zhang, C.; Hussain, I.; Tan, B. Novel POSS-based Organic−Inorganic Hybrid Porous Materials by Low Cost Strategies. *J. Mater. Chem. A* **2015**, *3*, 6542−6548.

(7) (a) Buyukcakir, O.; Seo, Y.; Coskun, A. Thinking Outside the Cage: Controlling the Extrinsic Porosity and Gas Uptake Properties of Shape-Persistent Molecular Cages in Nanoporous Polymers. *Chem. Mater.* **2015**, *27*, 4149−4155. (b) Alsbaiee, A.; Smith, B. J.; Xiao, L.; Ling, Y.; Helbling, D. E.; Dichtel, W. R. Rapid Removal of Organic Micropollutants from Water by a Porous β-Cyclodextrin Polymer. *Nature* **2016**, *529*, 190−194. (c) Talapaneni, S. N.; Kim, D.; Barin, G.; Buyukcakir, O.; Je, S. H.; Coskun, A. Pillar[5]arene Based Conjugated Microporous Polymers for Propane/Methane Separation through Host-Guest Complexation. *Chem. Mater.* **2016**, *28*, 4460−4466. (d) Zhang, Y.; Duan, J.; Ma, D.; Li, P.; Li, S.; Li, H.; Zhou, J.; Ma, X.; Feng, X.; Wang, B. Three-dimensional Anionic Cyclodextrin-Covalent Organic Frameworks. *Angew. Chem., Int. Ed.* **2017**, *56*, 16313−16317. (e) Shetty, D.; Jahovic, I.; Raya, J.; Ravaux, F.; Jouiad, M.; Olsen, J.; Trabolsi, A. An Ultra-absorbent Alkyne-rich Porous Covalent Polycalix[4]arene for Water Purification. *J. Mater. Chem. A* **2017**, *5*, 62−66. (f) Su, K.; Wang, W.; Li, B.; Yuan, D. Azo-Bridged

https://dx.doi.org/10.1021/acsomega.0c04248
ACS Omega 2020, 5, 28413−28424

Calix[4]-resorcinarene-Based Porous Organic Frameworks with Highly Efficient Enrichment of Volatile Iodine. *ACS Sustainable Chem. Eng.* **2018**, *6*, 17402−17409. (g) Yang, Y.; Zou, X.; Cui, P.; Zhou, Y.; Zhao, S.; Wang, L.; Yuan, Y.; Zhu, G. Porous Aromatic Frameworks for Size-Selective Halogenation of Aryl Compounds. *ACS Appl. Mater. Interfaces* **2017**, *9*, 30958−30963. (h) Zhao, Q.; Liu, Y. Tunable Photo-luminescence Behaviors of Macrocycle-containing Polymer Networks in the Solid-state. *Chem. Commun.* **2018**, *54*, 6068−6071. (i) Skala, L. P.; Yang, A.; Klemes, M. J.; Xiao, L.; Dichtel, W. R. Resorcinarene Cavitand Polymers for the Remediation of Halomethanes and 1,4-Dioxane. *J. Am. Chem. Soc.* **2019**, *141*, 13315−13319. (j) Ma, J.; Li, J.; Chen, Y.; Ning, R.; Ao, Y.; Liu, J.; Sun, J.; Wang, D.; Wang, Q. Cage Based Crystalline Covalent Organic Frameworks. *J. Am. Chem. Soc.* **2019**, *141*, 3843−3848. (k) Giri, A.; Hussain, W. M.; Sk, B.; Patra, A. Connecting the Dots: Knitting C-Phenylresorcin[4]arenes with Aromatic Linkers for Task-Specific Porous Organic Polymers. *Chem. Mater.* **2019**, *31*, 8440−8450.

(8) Moran, J. R.; Karbach, S.; Cram, D. J. Cavitands: Synthetic Molecular Vessels. *J. Am. Chem. Soc.* **1982**, *104*, 5826−5828.

(9) (a) Klemes, M. J.; Ling, Y.; Ching, C.; Wu, C.; Xiao, L.; Helbling, D. E.; Dichtel, W. R. Reduction of a Tetrafluoroterephthalonitrile-β-Cyclodextrin Polymer to Remove Anionic Micropollutants and Perfluorinated Alkyl Substances from Water. *Angew. Chem., Int. Ed.* **2019**, *58*, 12049−12053. (b) Xiao, L.; Ling, Y.; Alsbaiee, A.; Li, C.; Helbling, D. E.; Dichtel, W. R. β-Cyclodextrin Polymer Network Sequesters Perfluorooctanoic Acid at Environmentally Relevant Concentrations. *J. Am. Chem. Soc.* **2017**, *139*, 7689−7692. (c) Karoyo, A. H.; Wilson, L. D. Investigation of the Adsorption Processes of Fluorocarbon and Hydrocarbon Anions at the Solid-Solution Interface of Macromolecular Imprinted Polymer Materials. *J. Phys. Chem. C* **2016**, *120*, 6553−6568. (d) Yang, A.; Ching, C.; Easler, M.; Helbling, D. E.; Dichtel, W. R. Cyclodextrin Polymers with Nitrogen-containing Tripodal Crosslinkers for Efficient PFAS Adsorption. *ACS Materials Lett.* **2020**, *2*, 1240−1245.

(10) (a) Kim, D.; Kim, H.; Chang, J. Y. Designing Internal Hierarchical Porous Networks in Polymer Monoliths that Exhibit Rapid Removal and Photocatalytic Degradation of Aromatic Pollutants. *Small* **2020**, *16*, 1907555. (b) Li, H.; Meng, B.; Chai, S.; Liu, H.; Dai, S. Hyper-crosslinked β-Cyclodextrin Porous Polymer: An Adsorption-facilitated Molecular Catalyst Support for Transformation of Water-soluble Aromatic Molecules. *Chem. Sci.* **2016**, *7*, 905−909.

(11) (a) Shetty, D.; Jahovic, I.; Raya, J.; Asfari, Z.; Olsen, J.; Trabolsi, A. Porous Polycalix[4]arenes for Fast and Efficient Removal of Organic Micropollutants from Water. *ACS Appl. Mater. Interfaces* **2018**, *10*, 2976−2981. (b) Shetty, D.; Raya, J.; Han, D. S.; Asfari, Z.; Olsen, J.; Trabolsi, A. Lithiated Polycalix[4]arenes for Efficient Adsorption of Iodine from Solution and Vapor Phases. *Chem. Mater.* **2017**, *29*, 8968−8972. (c) Shetty, D.; Boutros, S.; Eskhan, A.; De Lena, A. M.; Skorjanc, T.; Asfari, Z.; Traboulsi, H.; Mazher, J.; Raya, J.; Banat, F.; Trabolsi, A. Thioether-Crown-Rich Calix[4]arene Porous Polymer for Highly Efficient Removal of Mercury from Water. *ACS Appl. Mater. Interfaces* **2019**, *11*, 12898−12903. (d) Shetty, D.; Boutros, S.; Skorjanc, T.; Garai, B.; Asfari, Z.; Raya, J.; Trabolsi, A. Fast and Efficient Removal of Paraquat in Water by Porous Polycalix[n]arenes (n = 4, 6, and 8). *J. Mater. Chem. A* **2020**, *8*, 13942−13945.

(12) Zhang, Q.; Catti, L.; Tiefenbacher, K. Catalysis Inside the Hexameric Resorcinarene Capsule. *Acc. Chem. Res.* **2018**, *51*, 2107−2114.

(13) (a) Zhao, Q.; Liu, Y. Macrocycle Crosslinked Mesoporous Polymers for Ultrafast Separation of Organic Dyes. *Chem. Commun.* **2018**, *54*, 7362−7365. (b) Jie, K.; Zhou, Y.; Sun, Q.; Li, B.; Zhao, R.; Jiang, D.; Guo, W.; Chen, H.; Yang, Z.; Huang, F.; Dai, S. Mechanochemical Synthesis of Pillar[5]quinone Derived Multimicroporous Organic Polymers for Radioactive Organic Iodide Capture and Storage. *Nat. Commun.* **2020**, *11*, 1086.

(14) Pyzer-Knapp, E. O.; Thompson, H. P. G.; Schiffmann, F.; Jelfs, K. E.; Chong, S. Y.; Little, M. A.; Cooper, A. I.; Day, G. M. Predicted Crystal Energy Landscapes of Porous Organic Cages. *Chem. Sci.* **2014**, *5*, 2235−2245.

(15) Wang, Z.; Ma, H.; Zhai, T.; Cheng, G.; Xu, Q.; Liu, J.; Yang, J.; Zhang, Q.; Zhang, Q.; Zheng, Y.; Tan, B.; Zhang, C. Networked Cages for Enhanced CO_2 Capture and Sensing. *Adv. Sci.* **2018**, *5*, 1800141.

(16) (a) Rowan, S. J.; Cantrill, S. J.; Cousins, G. R. L.; Sanders, J. K. M.; Stoddart, J. F. Dynamic Covalent Chemistry. *Angew. Chem., Int. Ed.* **2002**, *41*, 898−952. (b) Jin, Y.; Yu, C.; Denman, R. J.; Zhang, W. Recent Advances in Dynamic Covalent Chemistry. *Chem. Soc. Rev.* **2013**, *42*, 6634−6654.

(17) Zhu, Q.; Wang, X.; Clowes, R.; Cui, P.; Chen, L.; Little, M. A.; Cooper, A. I. 3D Cage COFs: A Dynamic Three-Dimensional Covalent Organic Framework with High-Connectivity Organic Cage Nodes. *J. Am. Chem. Soc.* **2020**, *142*, 16842−16848.

(18) (a) Pallavi, P.; Bandyopadhyay, S.; Louis, J.; Deshmukh, A.; Patra, A. Soluble Conjugated Porous Organic Polymer: Efficient White Light Emission in Solution, Nanoparticles, Gel and Transparent Thin Film. *Chem. Commun.* **2017**, *53*, 1257−1260. (b) Bandyopadhyay, S.; Kundu, S.; Giri, A.; Patra, A. A smart Photosensitizer Based on a Red Emitting Solution Processable Porous Polymer: Generation of Reactive Oxygen Species. *Chem. Commun.* **2018**, *54*, 9123−9126.

(19) Alzate-Sánchez, D. M.; Smith, B. J.; Alsbaiee, A.; Hinestroza, J. P.; Dichtel, W. R. Cotton Fabric Functionalized with a β-Cyclodextrin Polymer Captures Organic Pollutants from Contaminated Air and Water. *Chem. Mater.* **2016**, *28*, 8340−8346.

https://dx.doi.org/10.1021/acsomega.0c04248
ACS Omega 2020, 5, 28413−28424